

# The treatment of TRISO-coated particles with CF<sub>4</sub> in a low temperature plasma

\*Izak J. van der Walt<sup>1</sup>, Johann T. Nel<sup>1</sup>, Philippus L. Crouse<sup>2</sup>, Arnold A. Jansen<sup>1</sup>,  
Sipho J. Kekana<sup>1</sup>

<sup>1</sup>*The South African Nuclear Energy Corporation Ltd. (Necsa), P.O. Box 582, Pretoria, 0001, South Africa.*

*Department of Chemical Engineering, University of Pretoria, Lynnwood Road, Pretoria 0001, South Africa.*

\* Corresponding author: Izak J. van der Walt,

e-mail: [jaco.vanderwalt@necsa.co.za](mailto:jaco.vanderwalt@necsa.co.za)

Address: P.O Box 582, Pretoria, 0001, South Africa

Tel: (+27) 12 305 3216

Cell: (+27) 82 807 5630

Fax: (+27) 12 305 3197

## Abstract

An alternative recovery method to the mechanical crushing of off-specification tri-structural-isotropic (TRISO) coated fuel microspheres is demonstrated. It is shown that the inert SiC layer can be completely removed by etching with the active fluorine species from an inductively coupled radio-frequency CF<sub>4</sub> glow-discharge impinging a static bed from the top, at a working pressure of 1 kPa. At this pressure mass transport does not have a rate limiting role and the chemical reaction itself is rate determining. A treatment time of roughly four hours is required for the conditions reported here.

## Key words:

*Silicon carbide, etching, plasma, fluorine, nuclear waste, TRISO, carbon tetrafluoride*

# 1 Introduction

Generation IV high temperature nuclear reactors are preferentially fuelled by so-called TRISO (tri-structural-isotropic) coated uranium oxide particles [1,2,3]. The particle structure is schematically presented in Figure 1.

The  $\text{UO}_2$  kernels (0.5 mm) are consecutively coated with a porous carbon buffer layer ( $\sim 95 \mu\text{m}$ ), followed by the inner pyrolytic carbon (IPyC) layer ( $\sim 40 \mu\text{m}$ ), a high density silicon carbide (SiC) barrier layer ( $\sim 35 \mu\text{m}$ ) and an outer pyrolytic carbon (OPyC) layer ( $\sim 40 \mu\text{m}$ ). The silicon carbide layer provides containment for the radionuclides that are formed during fuel burn-up [4]. The outer diameter of the average coated particles is 0.92 mm. In PBMR fuel the coated particles are further embedded in a graphite sphere, or “pebble”, with an outer diameter of 60 mm.

In the conventional recovery process off-specification coated particles are mechanically cracked to expose the uranium oxide kernel for wet chemical treatment [4]. An alternative route to recover the uranium kernel with minimum damage, ready for re-coating, has been investigated in this work. The outer carbon layer (OPyC) can be removed by high temperature air oxidation to expose the SiC layer. This layer is inert to almost all chemical processes including high-temperature oxidation. Fluorine-containing glow discharge plasmas are widely used for etching in the microelectronics industry [5,6]. Such a plasma process for removal of the SiC layer offers an alternative to wet processing. Etching with a carbon tetrafluoride ( $\text{CF}_4$ ) glow discharge is described here and a kinetic model for the process is proposed.

## 2 Experimental

### 2.1 General experimental procedure

In this study TRISO coated zirconium oxide particles were used as surrogate High Temperature Reactor (HTR) fuel kernels. Samples for etching were prepared by heating the particles overnight at  $1\,000^\circ\text{C}$  in air to remove the OPyC layer and expose the SiC layer. Samples of these particles were then exposed to the afterglow of a non-thermal RF-induced  $\text{CF}_4$  discharge in a tubular borosilicate glass reactor. The

equipment was leak tested before each run. A schematic process flow diagram is presented in Figure 2.

The CF<sub>4</sub> glow discharge plasma was generated with an induction coil powered by a 1.5 kW 13.56 MHz RF generator. The system pressure was kept at about 1 kPa by a vacuum pump exhausting through a scrubber. The CF<sub>4</sub> flow was maintained at 7.2 g h<sup>-1</sup>.

The total off-gas stream from the process was drawn through a liquid nitrogen cooled trap and later analyzed by gas chromatography-mass spectrometry (GC-MS) on a 50 m *Porapak Q* capillary column.

## 2.2 Determination of the process kinetics

In initial experiments the etch rate was determined as a function of distance below the plasma glow. As expected the highest rate was found directly below the plasma and this position was selected as optimum for further experiments. From the mass loss data at this position, the degree of dissociation of was estimated to be better than 2%. This we define as the number of fluorine atoms available per molecule of CF<sub>4</sub>.

In a second series of experiments 0.5 g samples of particles were progressively exposed directly below the plasma for an hour per run up to a total of 5 hours reaction time. The feed rate of CF<sub>4</sub> and the reactor pressure were kept constant at 7.2 g h<sup>-1</sup> and 1 kPa, respectively. The plasma enthalpy was maintained at  $2.7 \times 10^7$  J kg<sup>-1</sup>.

The total sample (initially about 520 particles) was weighed before and after each hour of exposure. A number of particles (typically 12) were removed after each run and the residual SiC layer thickness determined by SEM. The remainder of the sample was weighed and returned to the reaction chamber for the next run. The total exposed area not only decreased due to etching, but also due to sampling; calculation of the specific loss rate was corrected accordingly. The results are presented in Table 1.

### 3 Results and discussion

Species observed in the off-gas stream apart from  $\text{CF}_4$  were mainly  $\text{SiF}_4$ ,  $\text{C}_3\text{F}_6$ ,  $\text{C}_4\text{F}_8$ , and  $\text{CO}_2$ . Some presence of hydrogen substitution was evident. A flaky white solid found on the inner wall of the borosilicate glass reactor was identified by XRD analysis as sodium aluminium fluoride. This is consistent with fluorination of the reactor wall as could be expected. The origin of the hydrogen responsible for the formation of *e.g.*  $\text{C}_2\text{H}_2\text{F}_4$ , found in the off-gas is uncertain. An explanation that can be offered at present is the presence of hydrocarbon gas residues trapped in the SiC layer during the coating process. Since the system was leak tested before each run the presence of air and water vapour can be discounted. Increased yields of  $\text{C}_3\text{F}_6$ ,  $\text{C}_2\text{H}_2\text{F}_4$  and  $\text{C}_4\text{F}_8$  observed during the fifth hour of treatment can be ascribed to the inner carbon layers becoming exposed and available in stoichiometric excess, leading to the formation of the unsaturated fluorocarbons [7].

A SEM image of a typical untreated coated particle is shown in Figure 3 and images illustrating the progression of the process are presented in Figure 4 to Figure 8.

After 4 hours of treatment there is evidence that in some cases the SiC layer was unevenly etched, exposing the Inner Pyrolytic Carbon (IPyC) layer (Figure 7). Two possible explanations come to mind: (1) the particles do not pack randomly in the bed upon re-introduction to the reactor, leaving one side preferentially exposed to the upstream gas flow, or, (2) residual or induced stress in the SiC layer causing accelerated etching. After 5 hours of exposure (Figure 8) the SiC layer was completely removed. The etching rate of the IPyC differs from that of the SiC as can be deduced from the increased mass loss during hour 5 (Figure 9).

The specific mass loss rate was obtained by calculating the particle surface area from particle diameter, layer thickness, density data and the estimated number of particles obtained from sample mass. The number of particles removed after each etching cycle was estimated and accounted for by the calculated mass loss per particle and the mass of the sample removed. The sample mass loss rate per run is plotted in Figure 9.

## 4 Process model

Various gas-solid kinetic models assume direct proportionality between reaction rate and available surface area [8]. Figure 10 below demonstrates that the assumption holds for this case, and that a model can be selected accordingly.

Two Stokes approximations for small shrinking particles [8] were deemed to be most appropriate for kinetic modelling, *viz.* for control by the chemical reaction itself, and by diffusion through the static gas film surrounding each particle. The stoichiometric coefficient for the solid,  $b$  (Equations 3, 5), is based on Equation 1 below.

$$F + \frac{1}{8}SiC = \frac{1}{8}SiF_4 + \frac{1}{8}CF_4 \quad (1)$$

The Stokes approximation for a reaction control mechanism is

$$\frac{t}{\tau} = 1 - (1 - X_{SiC})^{1/3} \quad (2)$$

where

$$\tau = \frac{\rho_{SiC}R_0}{bkC_F} \quad (3)$$

In the case of a gas-film diffusion control the relationships are given by

$$\frac{t}{\tau} = 1 - (1 - X_{SiC})^{2/3} \quad (4)$$

and

$$\tau = \frac{\rho_{SiC}R_0^2}{2bDC_F} \quad (5)$$

The degree of conversion of the solid,  $X_{SiC}$ , is found from Equation 6

$$X_{SiC} = 1 - \frac{M_t}{M_0} \quad (6)$$

The variables in Equations 2 to 6 are defined as:

$t$  = reaction time (h),

$\tau$  = time for complete reaction (h),

$X_{SiC}$  = degree of conversion of the solid,

$M_0$  = initial particle mass (kg),

$M_t$  = residual particle mass (kg) after time  $t$ ,

$\rho_{SiC}$  = SiC layer density ( $3.15 \text{ kg m}^{-3}$ ),

$R_0$  = initial diameter of the particle, or, in this case the SiC layer ( $8.62 \times 10^{-4} \text{ m}$ ).

$b$  = stoichiometric coefficient for the solid SiC,

$k$  = reaction constant ( $\text{m s}^{-1}$ ),

$D$  = the diffusion coefficient ( $\text{m}^2 \text{ s}^{-1}$ ), and

$C_F$  = concentration of the gaseous reactant ( $\text{kg m}^{-3}$ ).

In the case where only one of several layers was removed, completion of the process is assumed to be the point where the change in specific mass loss rate becomes zero. In practice however, it was found that the SiC layer was not etched uniformly towards the end of the process. This is evidenced by both the SEM image (Figure 7) and the increased mass loss during the last hour of etching (Figure 9). This increase can be ascribed to a faster etch rate for the progressively more exposed IPyC layer. By differentiating the second-order trend line equation and setting  $dy/dt = 0$  the time for complete reaction could be calculated ( $\tau = 3.9 \text{ h}$ ). This value can alternatively be obtained from a good model fit.

The values for  $1-(1-X_{SiC})^{1/3}$  and  $1-(1-X_{SiC})^{2/3}$  calculated from equations 2 and 4 are plotted as function of reaction time in Figure 11 and Figure 12 for the reaction control and diffusion control models respectively.

In fitting the data, the point at 4 hours was not used, since here it is clear that in many cases the IPyC coating is partially exposed, and the mass loss rate applies to a combination of SiC and carbon. It is obvious from a first comparison of trend line linearity that there is not much to choose between the two models, if this had to be the only criterion.

In order to obtain a value for the reaction constant and/or diffusivity from our data, *via* Equations (3) and (5), a value for the active gas species concentration is required. For example, Yang *et al.* [9] determined the concentration of F radicals in an atmospheric pressure low temperature CF<sub>4</sub>/argon plasma. According to their measurements the number density of CF<sub>4</sub> was  $3.1 \times 10^{17} \text{ cm}^{-3}$  and that of F atoms in the plasma was  $1.3 \times 10^{15} \text{ cm}^{-3}$ . The down-stream concentration of F atoms up to 20 mm away from the discharge was estimated to be  $1 \times 10^{15} \text{ cm}^{-3}$ . This relates to a degree of dissociation,  $\alpha = 3.22 \times 10^{-3}$ . Our value,  $\alpha \geq 2 \times 10^{-2}$ , was determined indirectly, from the etch rate data. We attribute the difference to our lower operating pressure. We use the inequality rather than equality sign to indicate that some of the fluorine atoms might have passed through the particle bed without reacting.

The reaction constant and diffusion coefficient obtained using this value for  $\alpha$  to calculate the fluorine radical concentration, are  $k \geq 0.6 \text{ m s}^{-1}$  and  $D \geq 2.4 \times 10^{-4} \text{ m}^2 \text{ s}^{-1}$  respectively. Typical room-temperature atmospheric-pressure diffusion coefficient values for gases range between  $10^{-5}$  and  $10^{-6} \text{ m}^2 \text{ s}^{-1}$  [10,11]. However, for the ideal, classical case, the diffusion coefficient is inversely proportional to the density and also a function of  $T^{3/2}$ , T being the absolute temperature [12]. Since the gas temperature is only marginally higher than room temperature in low-pressure glow discharges, a diffusion coefficient higher than typical by an order of magnitude is thus entirely feasible.

However, if gas-film diffusion were the rate limiting step, this would be independent of the etch mechanism. Since there is an obvious increase in the etch rate once the SiC has been consumed, the conclusion has to be that the chemical interaction between the fluorine radicals and the solid surface is rate determining; with the caveat that the process as reported here is very close to being limited by mass transport rate.

#### **4. Conclusions**

An alternative to mechanical crushing of off-specification TRISO coated particles has been investigated. It has been shown that the inert SiC layer can be completely removed by etching with active fluorine species from a CF<sub>4</sub> glow discharge plasma.

The outer and inner carbon layers can be removed by oxidation, which would leave the fuel kernel exposed and ready for re-coating.

The chemical reaction itself has been shown to be the rate controlling step, and a rate constant of  $k \geq 0.6 \text{ m s}^{-1}$  can be used for process development. However, should the concept be used for scaling and other reactor types, discretion should be used in selecting an operating pressure. Above the 1 kPa used in this work, mass transport phenomena could dominate the process rate.

### **Acknowledgements**

The authors wish to thank the Nuclear Energy Corporation of South Africa (Necsa) for permission to publish this work, and the South African National Research Foundation for support of the activities at the University of Pretoria.

### **References**

1. H. Nabielek, W. Schenk, W. Heit, A.W. Mehner, D.T. Goodin. *Journal of Nuclear Technology* 84 (1989) 62-80.
2. K. Minato, T. Ogawa, T. Koya, H. Sekino, T. Tomita. *Journal of Nuclear Materials* 279 (2000) 181-188.
3. F. Charollais, S. Fonquernie, C. Perrais, M. Perez, F. Cellier, G. Harbonnier. CEA and AREVA R&D on HTR fuel fabrication & presentation of the GAIA experimental manufacturing line, 2nd International Topical Meeting on HIGH TEMPERATURE REACTOR TECHNOLOGY, Beijing, CHINA, September 2004.
4. K.R. Ryan, I.C. Plumb. *Plasma Chem. Plasma Proc.* 6(3) (1986) 231.
5. M.A. Lieberman, A.J. Lichtenberg. *Principles of Plasma Discharges and Materials Processing*, Wiley, New York, 1994.
6. J. Swanepoel, R. Lombaard. Production of fluorocarbon compounds, US Patent 5611896, March 1997.
7. O. Levenspiel. *Chemical Reaction Engineering*, 3rd Ed, John Wiley & Sons, New York, 1999.
8. X. Yang, S.E. Babayan and R.F. Hicks. *Plasma Sources Sci. Technol.* 12 (2003) 484.



9. C.J. Geankoplis. Transport Processes and Unit Operations, Allyn and Bacon, Inc., Boston, 1978.
10. R.B. Bird, W.E. Stewart, E.N. Lightfoot. Transport Phenomena, 2nd edition, John Wiley and Sons, New York, 1960.
11. P.W. Atkins, J. de Paula, Atkins' Physical Chemistry, Oxford University Press, Oxford, 2006.

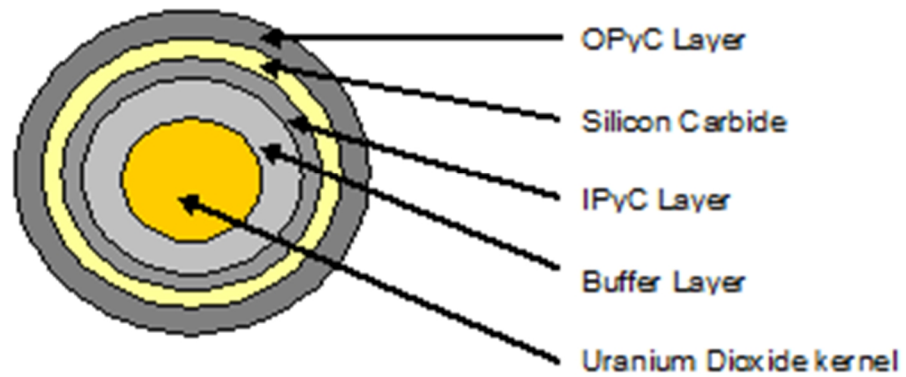


Fig. 1. Layer composition of a TRISO coated particle [1]. OPyC: Outer Pyrolytic Carbon layer; IPyC: Inner Pyrolytic Carbon layer.

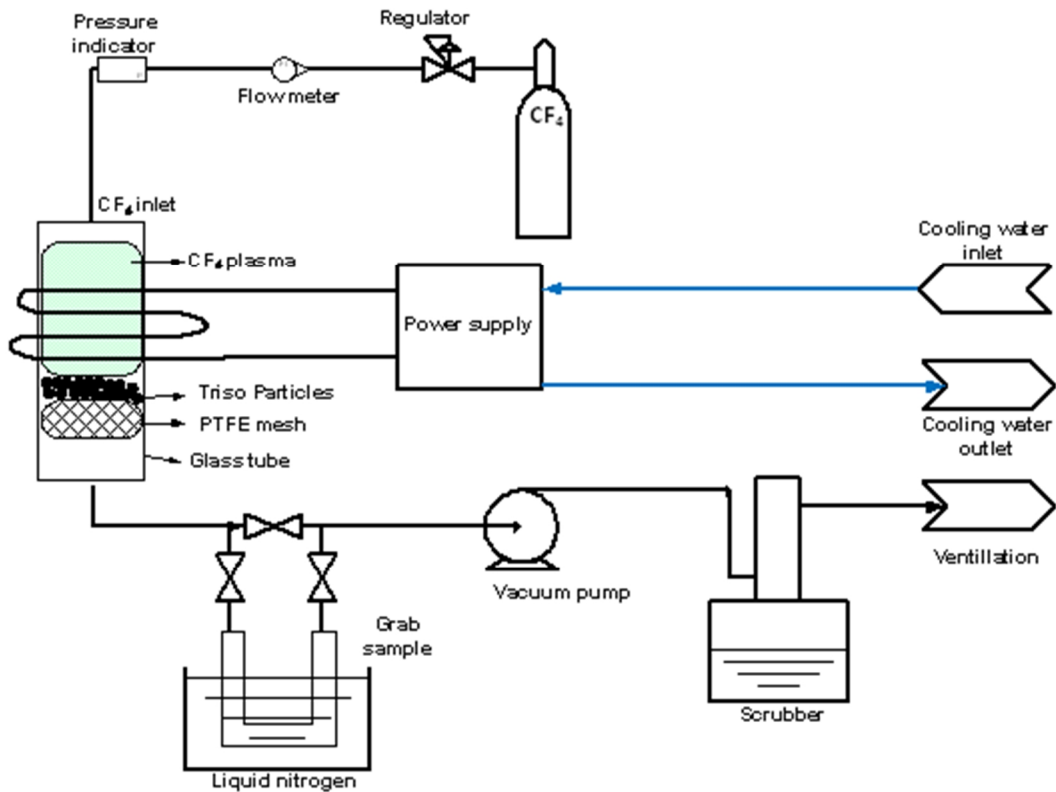


Fig. 2. Schematic process flow diagram.

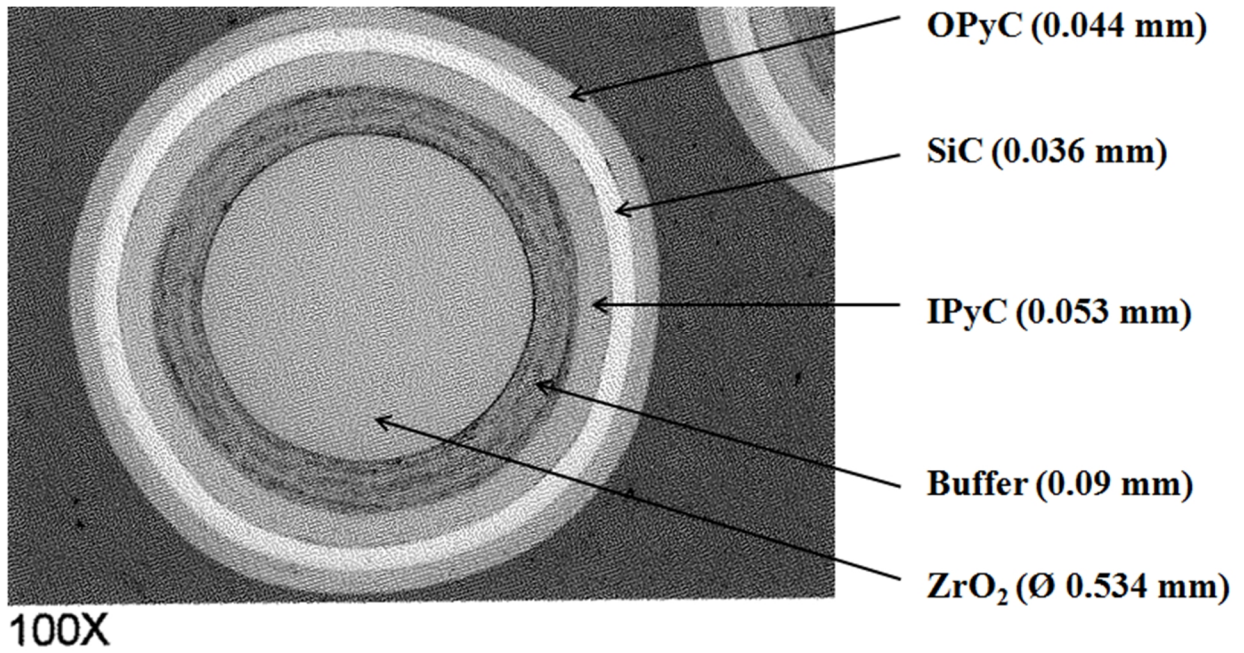


Fig. 3. Untreated coated particle.

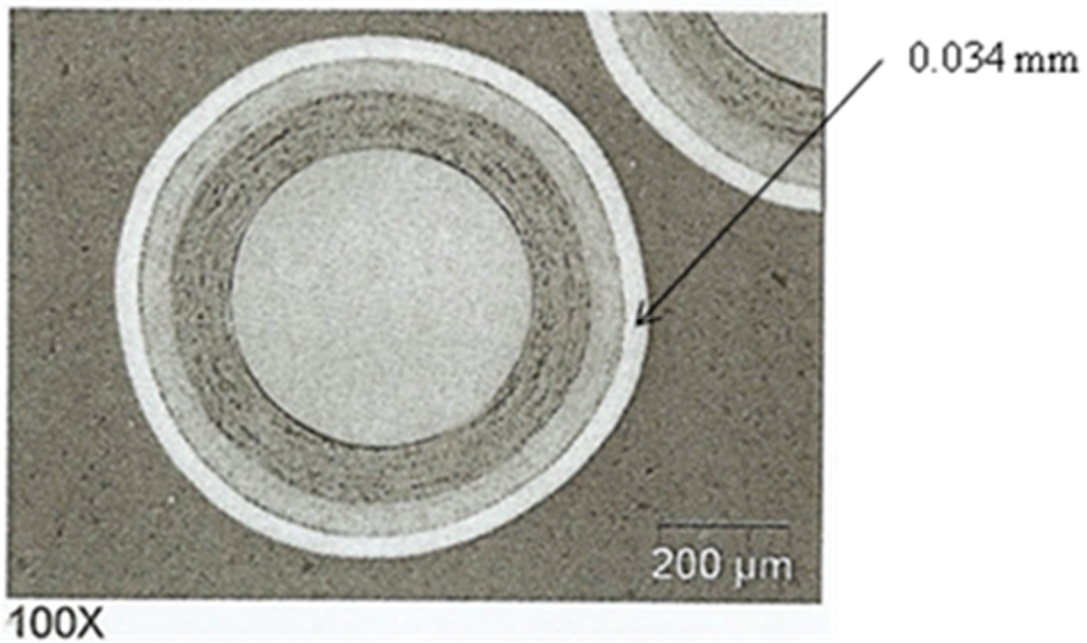


Fig. 4. Coated particle after 1 h exposure.

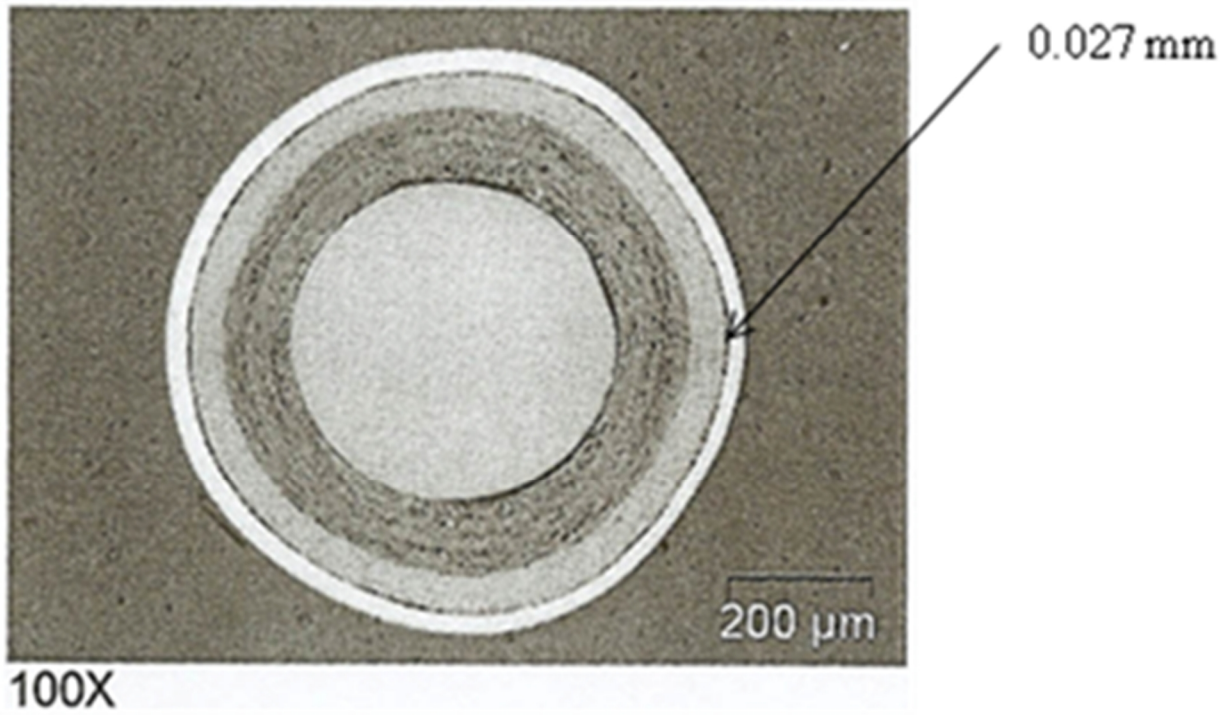


Fig. 5. Coated particle after 2 h exposure.

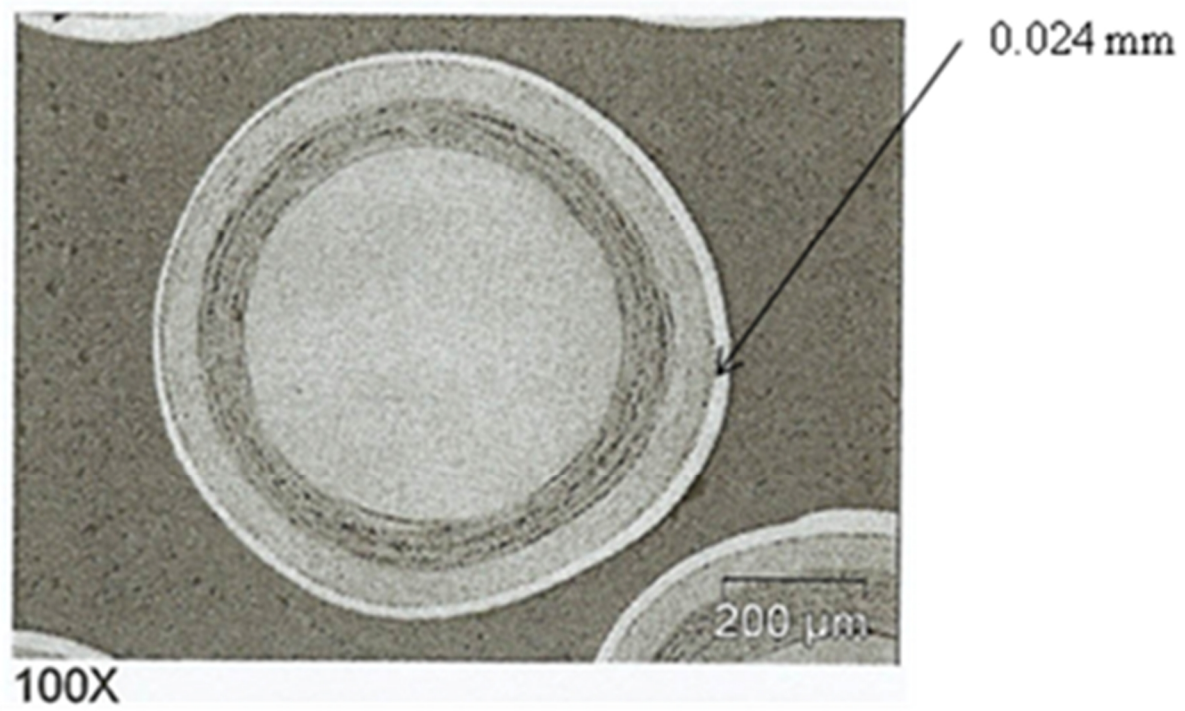


Fig. 6. Coated particle after 3 h exposure.



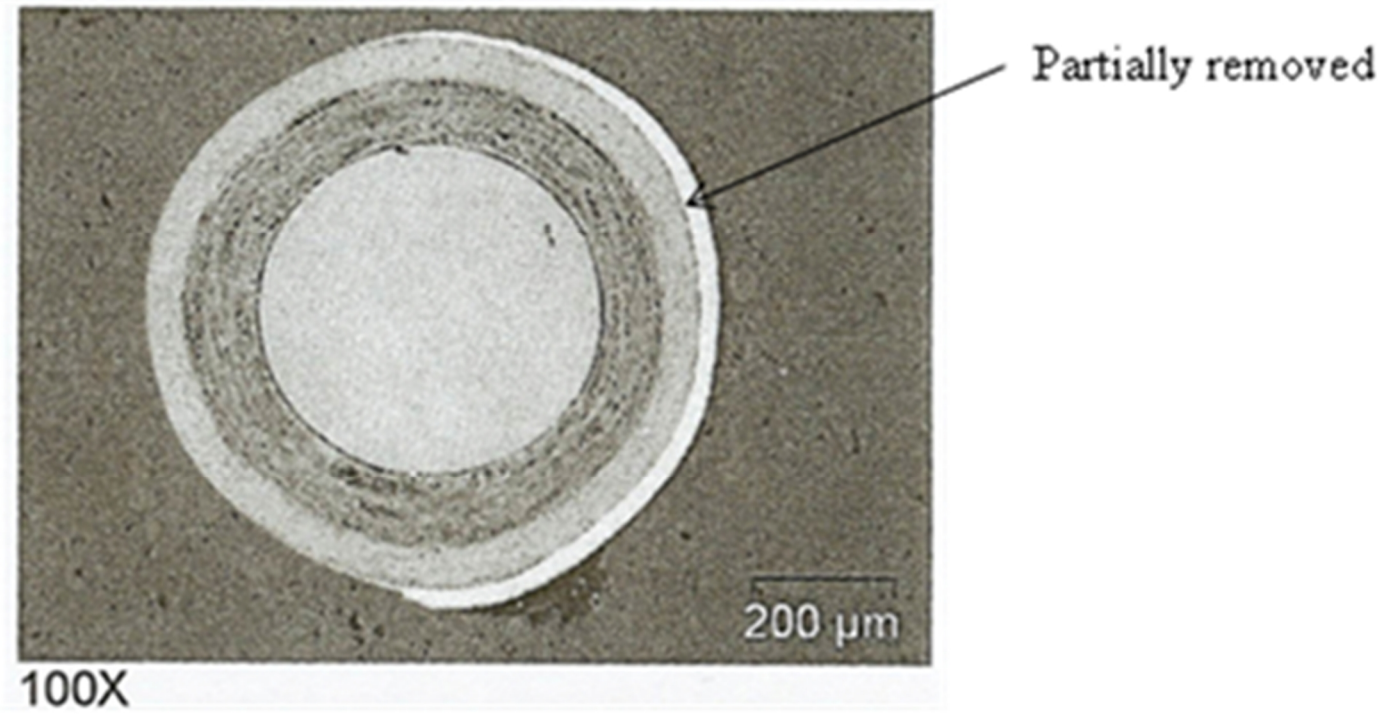


Fig. 7. Coated particle after 4 h exposure.

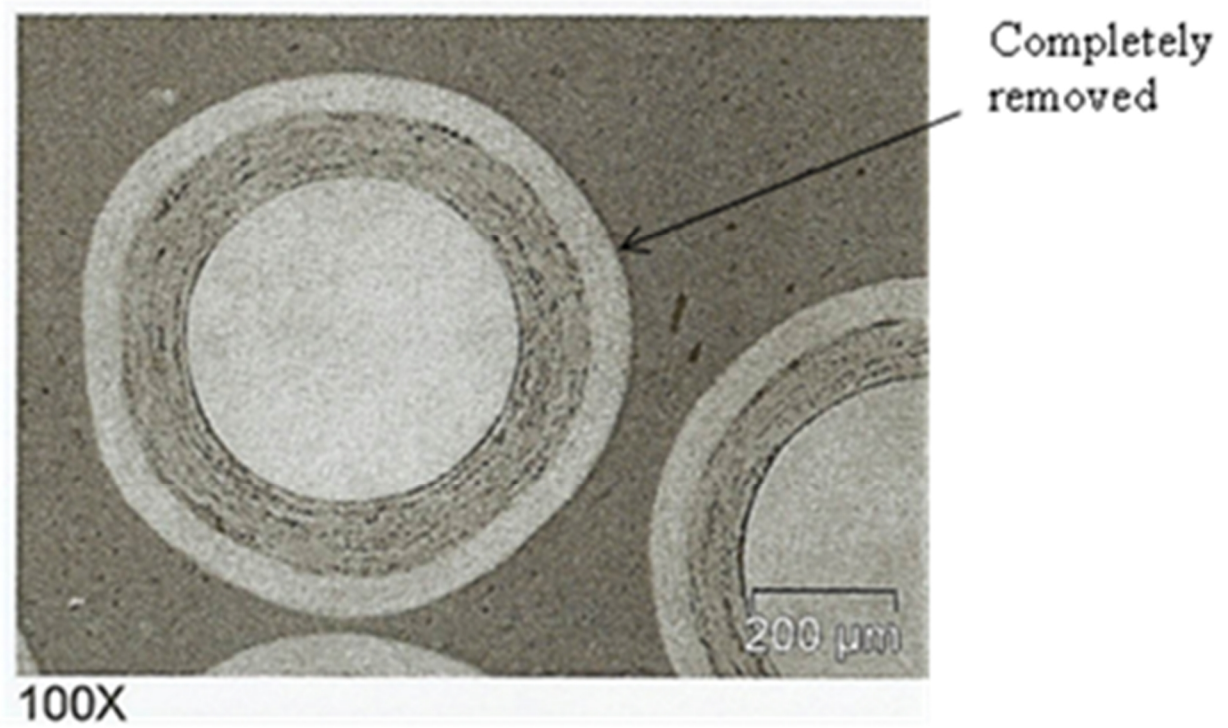


Fig. 8. Coated particle after 5 h exposure.

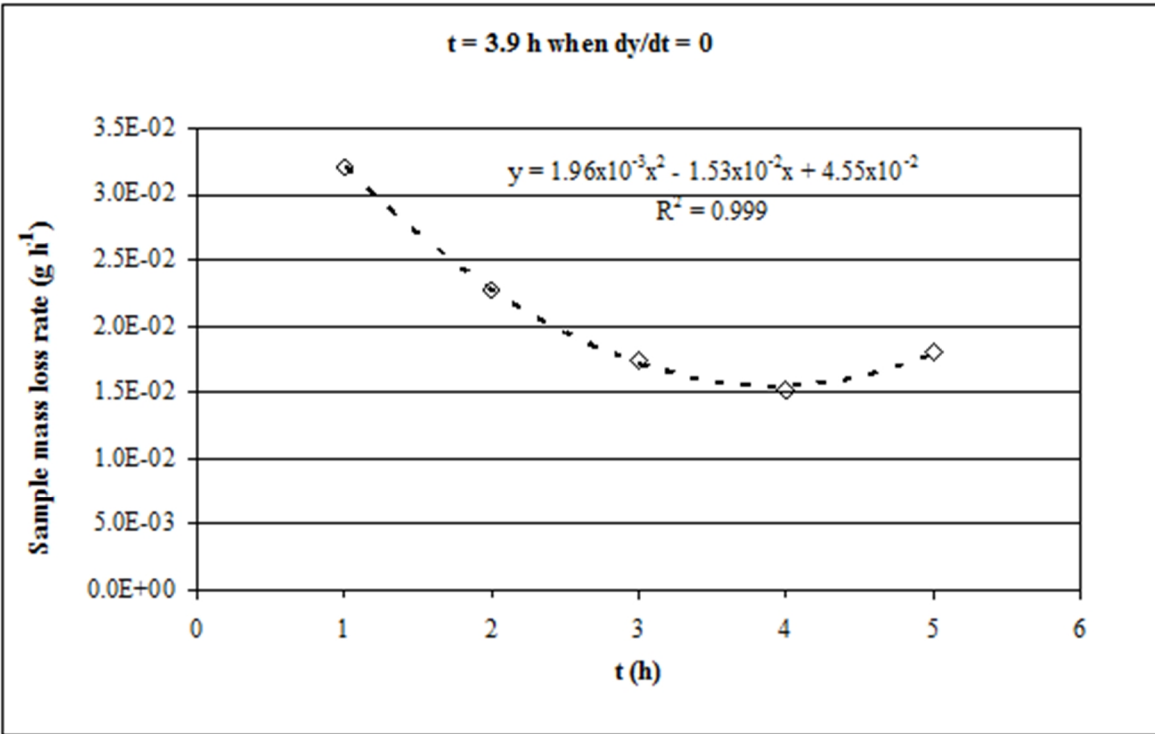


Fig. 9. Sample mass loss rate per run.

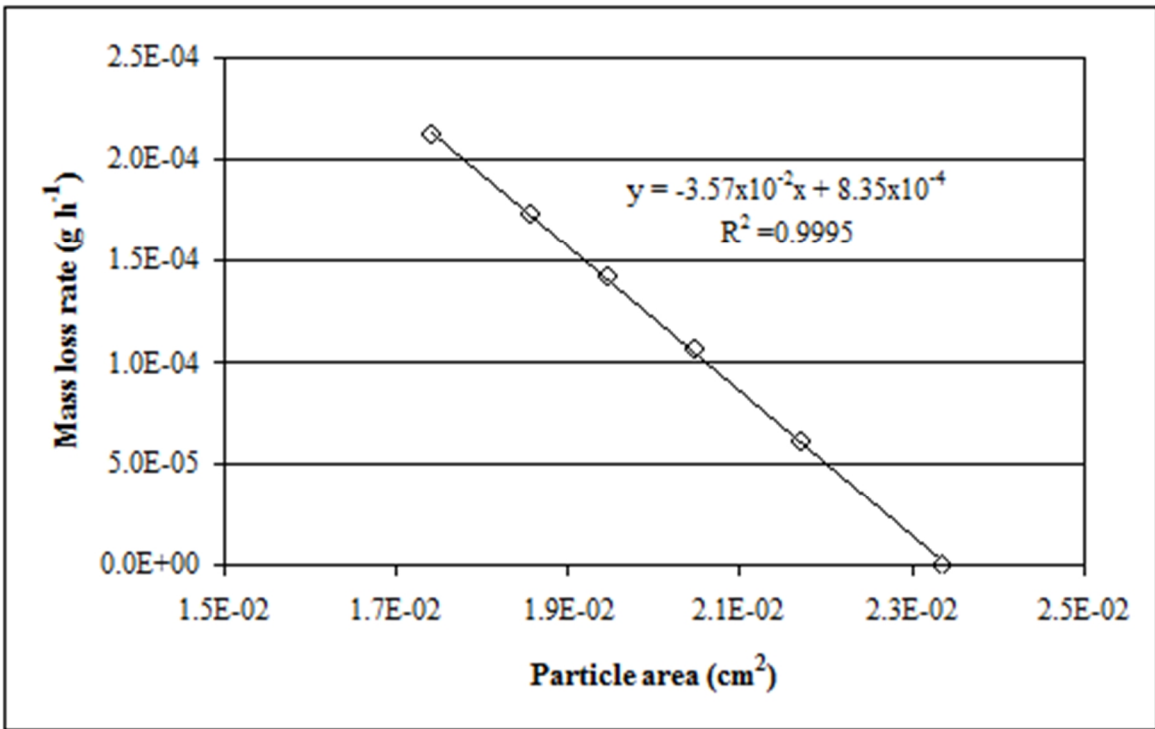


Fig. 10. Proportionality between SiC layer etch rate and area per particle.

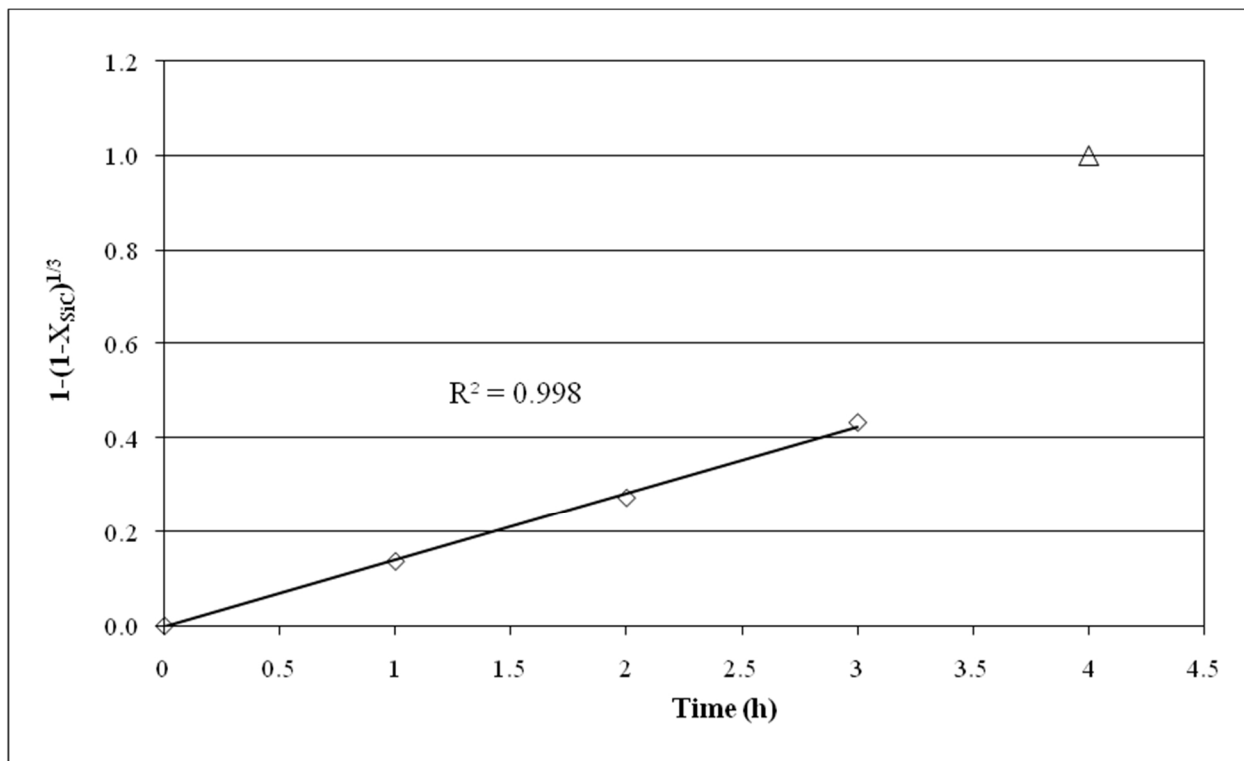


Fig. 11. Reaction-rate control model.

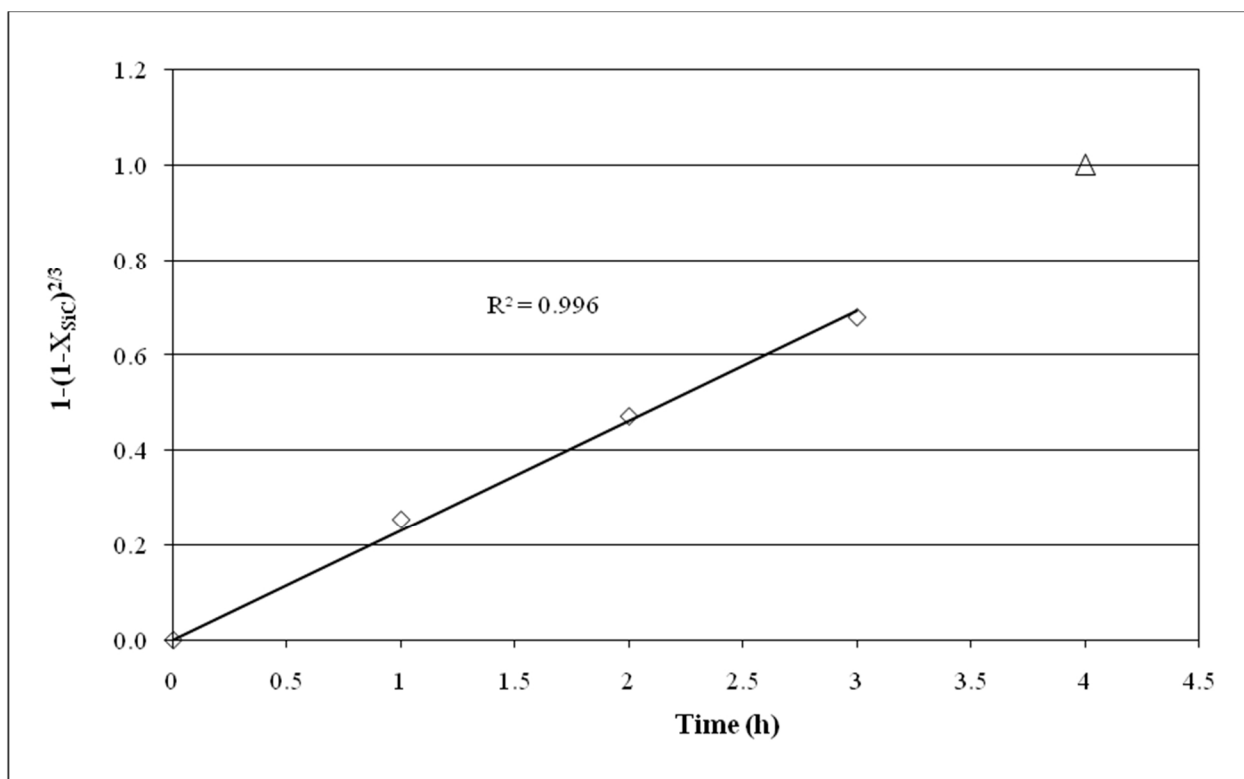


Fig. 12. Gas-film diffusion control model.